

Software Radio Development and Integration with a Small Unmanned Aerial Vehicle

Peter Stuckey,^{*} Richard Gable,[†] and Steve Peacock[‡]
Raytheon, Falls Church, Virginia 22042

Unmanned aerial vehicles (UAV) with high performance software radio relays will offer dramatic improvements to Situational Awareness and Command and Control for future warfighters. A key to this advancement is assured, reliable communications among all ground and air assets. This paper will describe the development of a compact, low power, high performance communications system for UAVs to enable high data rates in difficult environments, low probability of intercept/detection, and anti-jam capability. The radio is software programmable for compatibility with legacy waveforms and functions over 20 MHz to 3 GHz with both wide- and narrowband networking waveforms. The development of this system within the Defense Advanced Research Projects Agency Future Combat System framework, and integration with a small UAV is detailed.

I. Introduction

A GOAL of the Defense Advanced Research Projects Agency's (DARPA) Future Combat System - Communications (FCS-C) is to develop a means of assured battlefield communications and integrate the system with ground and airborne vehicles, including small unmanned aerial vehicles (UAV). UAVs are intended as both a data relay between ground nodes that do not have Line of Sight (LOS), and also to collect and distribute reconnaissance information. A system demonstration was conducted in August of 2003 showing the capability of maintaining networked communications between ground and air nodes in an adverse environment at the Orchard Training Area in Idaho.

This paper will provide a brief description of the FCS-C program, with emphasis on the limited payload capacity of a small UAV, which requires a small, high performance, assured communications system. A technical description of an innovative new communications system will be presented, including the integration of the system with the UAV and development of a new wideband networking waveform. The paper will conclude with a discussion of ongoing and future activity. A list of acronyms is provided at the end of the paper.

II. FCS-C Program

The FCS vision is of a network-centric, remotely deployable, highly distributed, highly maneuverable, highly robotic, brigade level force. Profoundly better situational awareness (SA) and command and control (C2) will be achievable by intra-cell networking of various sensors, weapons, and vehicles/units; and by networking these assets with internal cells, as well as with assets external to the brigade. This rich mesh adaptive network will provide the communications foundation for the tactical information grid that enables the FCS vision.¹

Table 1 lists several of the objectives DARPA has identified to achieve these goals. In August 2003 a system demonstration was conducted to verify that the communications system met these objectives, and that the system was at least at Technology Readiness Level 5 (TRL 5). Technology Readiness Levels are used to define system maturity, and range from TRL 0 (basic principles) to TRL 9 (flight proven). TRL 5 refers to breadboard validation of the system in the relevant environment.²

Received 17 December 2003; revision received 22 April 2004; accepted for publication 16 June 2004. Copyright © 2004 by the American Institute of Aeronautics and Astronautics, Inc. All rights reserved. Copies of this paper may be made for personal or internal use, on condition that the copier pay the \$10.00 per-copy fee to the Copyright Clearance Center, Inc., 222 Rosewood Drive, Danvers, MA 01923; include the code 1542-9423/04 \$10.00 in correspondence with the CCC.

^{*}7700 Arlington Blvd., pstuckey@raytheon.com. Senior Member AIAA.

[†]7700 Arlington Blvd., rgable@raytheon.com.

[‡]7700 Arlington Blvd., speacock@raytheon.com.

Table 1 FCS-C Low Band Objectives³

Operating Band <3 GHz (5 km, LOS)		
Data Rate	High throughput	10 Mbps
	LPD mode	200 kbps
Jammer Rejection	Spatial 45°	> 10 dB
	Temporal	> 40 dB
Latency	< 200 ms roundtrip	
Node Entry	< 10 seconds	

UAVs are critical to achieving the objectives of the FCS-C program. Air nodes will route data between nodes that do not have direct LOS, or are impaired by interferers. The air nodes also will carry sensors, and therefore will need high data rate capability, while the necessity for long loiter times will mean the communications payload will be limited in size, weight and power.

III. Ultra Comm System

Current military radios tend to suffer from one or more of the following drawbacks: large, power hungry, limited frequency coverage, poor multipath performance, low data rates, and/or limited waveform compatibility. The Ultra Comm system was designed to address each of those drawbacks. Ultra Comm is a compact, lightweight, scalable, communications system designed for broad frequency coverage, and assured communications in hostile environments. The core of the radio consists of three personal computer memory card international association (PCMCIA) form factor cards: the advanced digital receiver (ADR), Advanced Digital Transmitter (ADT), and the Digital Processing Engine (DPE). The small size of the core modules makes the system compatible with small tactical UAVs, while the architecture is designed for expansion to multi-band, and multi-channel configurations to accommodate the functions expected of larger UAVs. It is designed for continuous frequency coverage over 20 MHz to 3 GHz, and is software programmable for continuously variable adaptability to the known environment. It can transmit and receive instantaneous bandwidths up to 30 MHz, and can be programmed with multiple modulation formats and data rates. The system allows for data rates exceeding 10 Mbps in clear conditions. While in hostile environments, the radio can achieve Low Probability of Interception/Low Probability of Detection/Anti Jam (LPI/LPD/AJ) communications at reduced data rates.

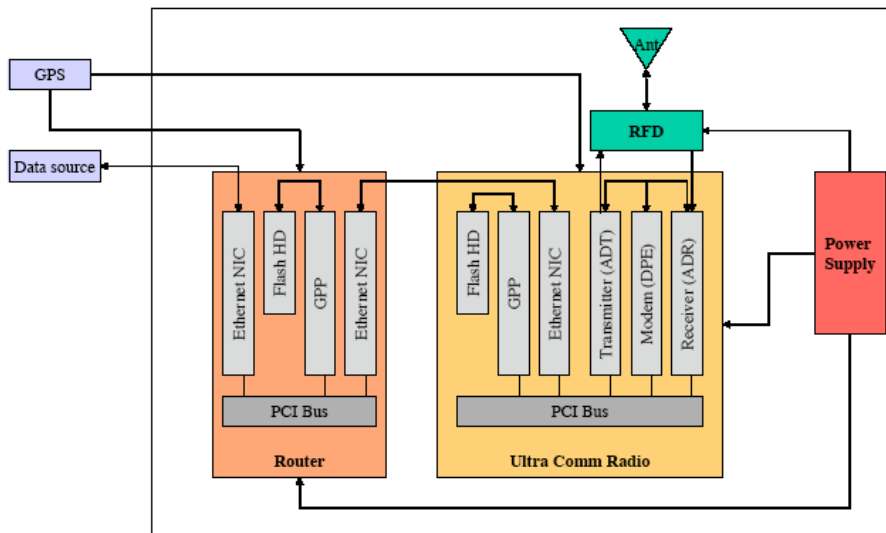


Fig. 1 Communications System Block Diagram.

The communications system (see Fig. 1) consists of a radio, RF (radio frequency) distribution, power supplies, antenna, global positioning system (GPS) source, and router. The radio (see Fig. 1 and Fig. 2) consists of a Receiver, Transmitter, Modem and General Purpose Processor mounted on a miniaturized peripheral component interconnect (PCI) back plane in a compact chassis. It is designed for small size, lightweight, high data rates, and software re-

programmability. Several innovative design solutions allowed the RF hardware to fit within the reduced Size, Weight and Power (SWAP) envelope of a small UAV. The processing power of the Digital Processing Engine (DPE), combined with the flexibility of the RF hardware enable a situation where bandwidth, center frequency, data rate, modulation format, range, signal to noise ration (S/N), and LPI/LPD/AJ characteristics can be varied with the changing environment.

Development of the radio and waveform was a primary focus of the development effort. Emphasis in the paper is placed on the core of the system: the ADR (Sec. III.A), ADT (Sec. III.B) and DPE (Sec. III.C). The RF distribution (Sec. III.D), antenna (Sec. III.E) and power supplies (Sec. V) are also briefly described, followed by the mechanical integration in Sec. VI. Section IV contains a description the wideband networking waveform that is currently implemented in the radio.

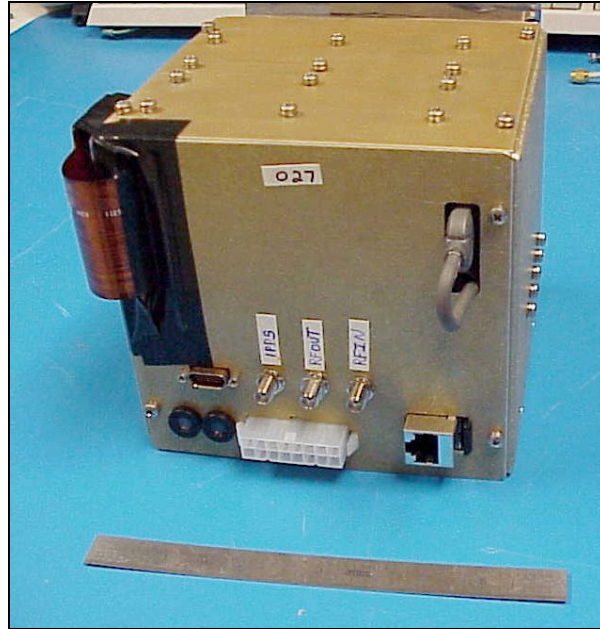


Fig. 2 UAV Radio.

A. Advanced Digital Receiver

The ADR is a wideband receiver built on a single 2.1” x 3.25” x 0.5” card. It covers the range of 20 MHz to 3 GHz, with instantaneous bandwidth up to 30 MHz. Typical spur free dynamic range into the Analog to Digital Converter is 70 dB, and it has 88 dB of distributed gain control, which results in a very large gain controlled dynamic range. The gain control of the ADR is adjusted dynamically by a digital automatic gain control (AGC) loop within the DPE. A block diagram of the ADR is shown in Fig. 3.

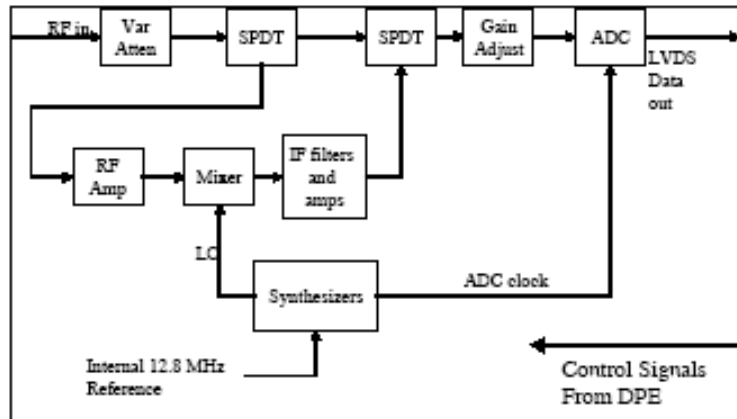


Fig. 3 ADR Block Diagram.

There are several enabling innovations that allowed the ADR to fit on a single card. A single conversion frequency plan eliminated the need of a second mix and second local oscillator (LO) generation, which saved considerable board area. Second, and key to enabling a single conversion, was the use of a high speed analog to digital converter (ADC) with a wide analog bandwidth. This ADC allowed direct sampling in VHF, and intermediate frequency (IF) sampling at higher frequencies. This ADC can sample up to 210 MSPS, though currently it is programmed for 102.4 MSPS. The third innovation was to use a single voltage controlled oscillator (VCO) scheme to generate the 3+ octaves of mixer LO. A summary of the ADR's capabilities is shown in Table 2.

Table 2 ADR Capabilities

Frequency	20 MHz – 3 GHz
Bandwidth	Up to 30 MHz
Gain	46 dB max
Gain control	88 dB
Tuning Speed	100 us
Phase Noise	-80 dBc/Hz @ 10 kHz
Sample Rate	Up to 210 MSPS

B. Advanced Digital Transmitter

The ADT, like the ADR, is built on a single 2.1" x 3.25" x 0.5" card. It also covers 20 MHz to 3 GHz, with instantaneous bandwidths up to 30 MHz. It utilizes a wide dynamic range, high-speed Digital to Analog Converter and a single mix frequency plan. The ADT has designed-in flexibility for power output control. Currently, this is optimized once for each platform configuration and fixed. However, the architecture accommodates dynamic transmit power control. A block diagram of the ADT is shown in Fig. 4.

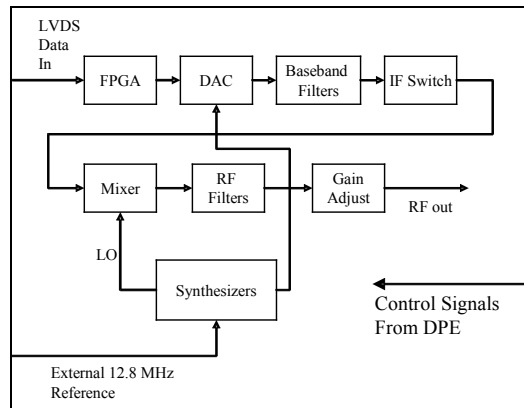


Fig. 4 ADT Block Diagram.

A plot of the ADT transmitting the AV-OFDM (orthogonal frequency division multiplexing) waveform is shown in Fig. 5. The waveform consists of 1024 carriers, each 25 kHz apart, in an instantaneous bandwidth of 25.6 MHz.

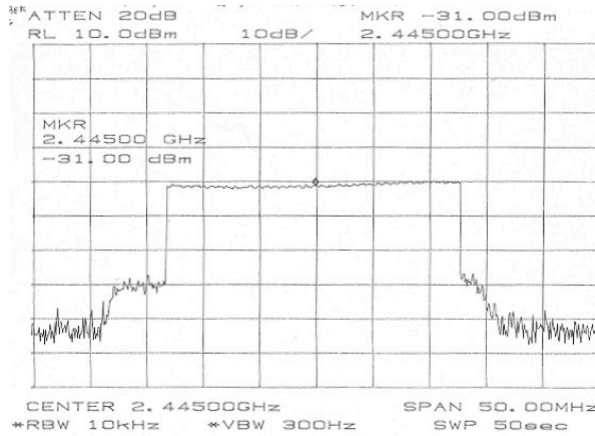


Fig. 5 AV-OFDM Spectrum From ADT.

A summary of the ADT’s capabilities is shown in Table 3.

Table 3 ADT Properties

Bandwidth	20 MHz – 3 GHz
Power out	Up to 30 MHz
Gain control	+4 dBm max at 2.4 GHz
Tuning Speed	60 dB
Phase Noise	100 us
Input Data Rate	-80 dBc/Hz @ 10 kHz
	Up to 160 MSPS

C. Digital Processing Engine

The DPE, like the ADR and ADT is built on a single PCMCIA form factor card. The DPE provides the processing power required to implement the communications waveform and also controls variable aspects of the ADR, ADT and RF distribution system (RFD) (gain control, frequency tuning, IF selection, T/R switching, power down modes). Low voltage differential signaling (LVDS) was chosen as the interface to the high speed ADC and digital to analog converter (DAC) to take advantage of superior common mode, ground bounce, and electro magnetic interference (EMI) characteristics of differential signaling. The DPE, in conjunction with the high IF ADC and DAC allows baseband processing to take place digitally. This considerably reduces the size and complexity of the analog hardware in the ADR and ADT. It essentially eliminates one mixer stage and associated filtering, and also eliminates I&Q modulators and demodulators. And of particular importance, performing these functions in the digital domain enables the radio to be adaptable in various performance dimensions under software control. The DPE is software configurable for compatibility with multiple waveforms.

AV-OFDM (see Sec. IV), in particular, requires considerable processing power. The heart of an OFDM (orthogonal frequency division multiplexing) waveform is the fast Fourier Transform (FFT) and inverse fast Fourier Transform (IFFT). In addition to performing FFTs and IFFTs, the DPE also implements forward error correction (FEC), interleaving, data randomization and feature suppression in the OFDM waveform.

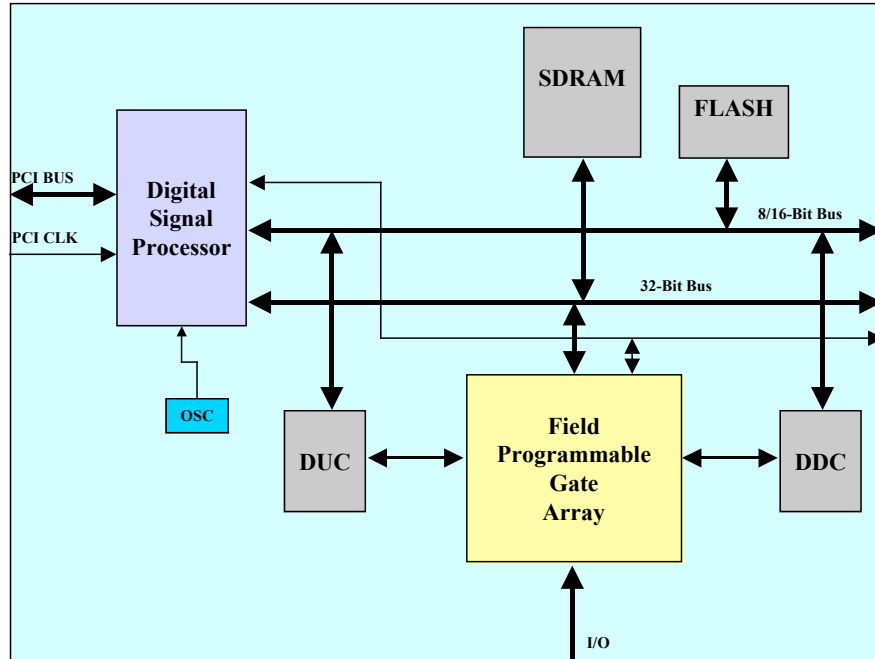


Fig. 6 DPE Block Diagram.

The DPE uses a 6 million gate Xilinx field programmable gate array (FPGA) and TI digital signal processor (DSP) for digital processing. Due to tight timing requirements, much of the AV-OFDM waveform was implemented in the FPGA. It is expected that legacy waveforms would be implemented using a combination of DSP and FPGA, although the DPE also includes commercial four-channel Digital-Up-Converter and Digital-Down-Converter application specific integrated circuits (ASIC) to efficiently support moderate bandwidth applications.

D. RF Distribution

The RFD consists of all the hardware between the antenna and the radio (see Fig. 7). For the 2003 demonstration, the RFD was constructed with all connectorized components and flexible coaxial cable (see Fig. 8). This is consistent with the intent of demonstrating a TRL 5 system, as described in Sec. II. The next step would be to integrate the RFD functions onto a PCMCIA form factor card for inclusion with the ADR, ADT, and DPE in the chassis. This would dramatically reduce the size and weight of the RFD.

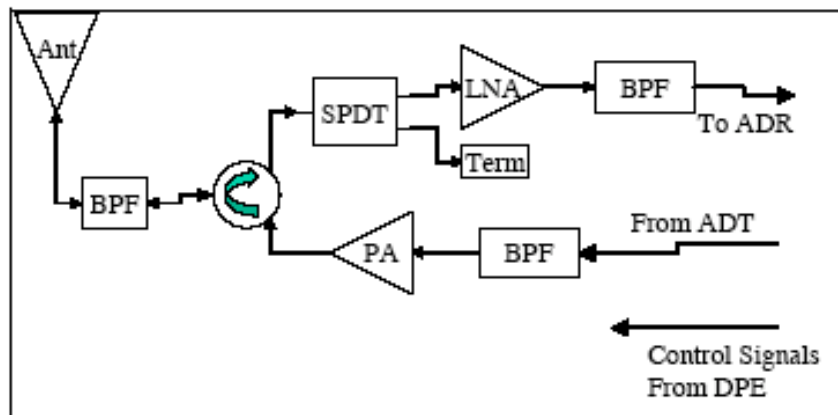


Fig. 7 RFD Block Diagram.

On the transmit side, the RFD filters the output of the ADT (which includes spurious output and LO feed-through), and amplifies the signal to a peak power of +33 dBm, then post-filters to remove power amplifier (PA) harmonics. On the Receive side the RFD filters out-of-band interferers, amplifies the weak receive (Rx) signal with

a low noise amplifier (LNA) and filters the output. Particular care was taken to minimize losses in the front end of the RFD. The RFD essentially sets the noise figure for the Rx path, and defines the output power for the transmit (Tx) path. The PA must be carefully designed to limit distortion due to the peaks produced by the OFDM waveform. Third order distortions are a particular concern since they can fall in-band and can lead to increased bit error rates. The RFD also attenuates LO re-radiation from the ADR and ADT for LPD.

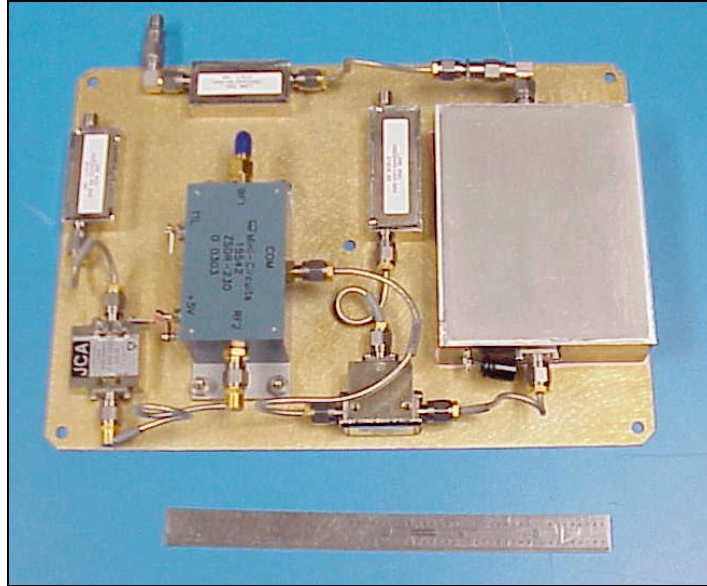


Fig. 8 Flight RFD.

A circulator was chosen over a T/R switch to provide low loss after the PA and before the LNA and also to reduce the number of power and control signals to the RFD. A low power commercial off-the-shelf (COTS) RF switch was placed after the circulator to provide additional Tx to Rx port isolation. Future versions of the RFD would be integrated in a PCMCIA form-factor card.

E. Antenna

The antenna chosen for the demonstration is a small (1 3/4" diameter, 3" high) commercial antenna made by Mobile Mark, shown in Fig. 9. It is designed primarily for wireless local area network (WLAN) applications in the 2.4 GHz industrial, scientific, and medical (ISM) band. The antenna has an omni radiation pattern, with 2.5 dBi maximum gain, and 2:1 max voltage standing wave ratio (VSWR) over 2400 – 2485 MHz. A COTS antenna was chosen for this demonstration because the focus at this stage of development was on proving the radio, waveform, and networking. This particular antenna was chosen for this application due to its availability, small size, low cost and rugged design. The antenna was located within the body of the UAV, and was ~1 ft from the RFD.



Fig. 9 UAV Antenna.

F. Lab Testing

Lab testing was conducted on the radio, flight power supply and RFD. The tests were conducted through cables using high power RF attenuators to simulate path loss. Digital gain and ADT signal levels were optimized for the UAV RFD. ADR attenuation was controlled by the AGC loop (which also was optimized for the UAV).

Integration testing revealed that low levels of a sinusoidal low-frequency noise component on the 5 V analog input were degrading receiver performance. The cause of this noise was related to dynamic load activity on other modules coupling into the 5 V modules. Connecting an electrolytic capacitor across the output terminals reduced the amplitude of this noise component. System performance after adding this capacitor is essentially identical to performance when it is powered from a bank of quiet linear supplies. A summary of the system level results is shown below in Table 4 (note that values in Table 4 does not include antenna gain).

Table 4 System Test Results

High Data Rate (10 Mbps - data) Mode	
Power Out of RFD	+30 dBm average +34 dBm peak
Max Atten for No Bit Errors	115 dB
Min Atten for No Bit Errors	<30 dB
Noise figure	8.5 dB

Based on these results we can estimate the communications range for the UAV in line of sight (LOS) conditions using equation 1. PL refers to the total path loss for the system, and is derived from the Max Attenuation value by including antenna gain as well as cable loss to/from the antenna. F refers to the 2.4 GHz ISM band. Thus plugging into equation 1, the predicted range is approximately 8 km in clear conditions.

$$\text{Range} = 10^{(PL/20)} * c / (4 * \pi * F) \quad (1)$$

For systems where one end of the link can afford higher antenna gain (large air or ground vehicle for example) the range will be correspondingly longer.

IV. □ Waveform

As part of the FCS-C program, we have developed a waveform for enhanced operation in adverse environments. This waveform is adaptive vector orthogonal frequency division multiplexing (AV-OFDM). AV-OFDM can be operated in many different modes to optimize data rate, S/N, range, bandwidth and LPI/LPD/AJ features. OFDM will not be described in detail in this paper, but in general terms it is a multiple carrier waveform that takes advantage of properties of the FFT and IFFT to efficiently occupy a given bandwidth. The reader is referred to Ref. 4 for more information on OFDM. In our system the instantaneous bandwidth is 25.6 MHz, although lower bandwidth modes can be used, and channels can be arbitrarily excised to maximize spectral efficiency by sharing the spectrum with other radios operating in the same frequency band. OFDM waveforms are well known for their advantage in heavy multi-path environments (which is a particular concern in urban environments) due to the reduced bandwidth of each individual carrier. However, the cost of this waveform choice is a wide dynamic range linear signal path for both RF transmit and receive and the digital processing.

A drawback to multiple carrier waveforms, which must be taken into account at all levels of the design, is the high peak to average power ratio (PAPR) of the signal. The PAPR scales directly with the number of carriers. For our implementation, an ideal undistorted linear system would result in a PAPR of ~30 dB. Our solution is to optimize the amount of digital and analog gain to maximize communications range, while significantly reducing PAPR. This creates some unavoidable distortion, which results in occasional bit errors. However, the channel includes Reed-Solomon Forward Error Correction Coding to correct transmission errors (either from peak limiting or RF channel effects). The type and strength of FEC is programmable. For the 2003 demonstration two Reed-Solomon encoding schemes were implemented. The high data rate mode (10 Mbps before FEC) included strong Reed-Solomon (RS) encoding (31,16) to correct multiple symbol errors per block, while the LPI/AJ mode used a modified, lower throughput (200 kbps before FEC) waveform which required weaker RS encoding. Data interleaving is used to reduce the effect of short duration fades and impaired frequencies.

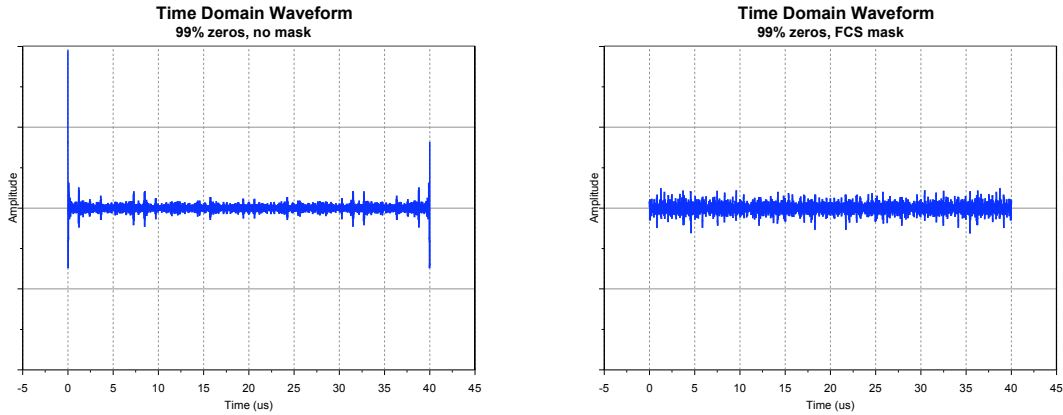


Fig. 10 Time Domain OFDM With and Without Randomization.

Simple clipping of OFDM peaks is not a complete solution however, because data patterns that create a large peak that when clipped effectively lower the signal to noise ratio on transmit - resulting in more bit errors. This could occur through highly repetitive data patterns, or could be induced by the communications protocol itself (such as zero stuffing). To combat this we have developed a data pattern randomization mask to suppress large excursions even with largely homogenous or cyclical data. The left hand chart of Fig. 10 shows the time domain representation of an unrandomized, unclipped OFDM waveform, notice the extremely large peak at the beginning of transmission. A significant portion of the signal energy is concentrated in one large peak at the start of the slot, which if clipped would significantly degrade the S/N of the signal. The other alternative is to back off the PA enough so the peak can pass unclipped, the drawback with this approach is that it severely reduces the average signal which also significantly degrades S/N. The right hand chart of Fig. 10 shows the same waveform passed through our randomization mask. The signal power is spread much more uniformly over the time of the slot. The result is longer communication range for a given PA power rating (see Fig. 11).

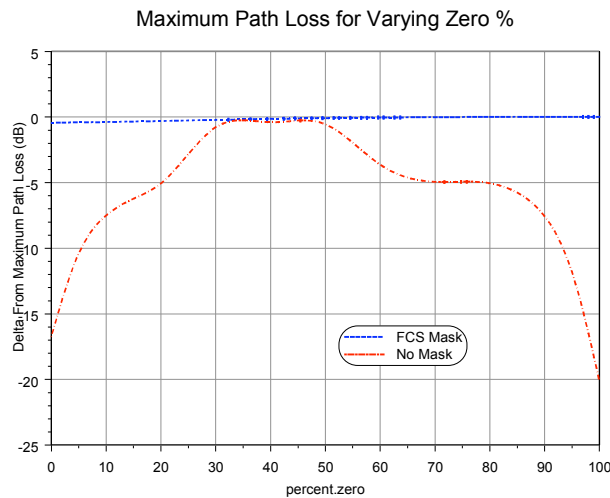


Fig. 11 Path Loss With and Without Randomization Mask.

V. □ Power Supplies

The power supply conditions power from the payload battery, supplying all the voltages required by the entire payload. Key design criteria were size, weight and efficiency. Program schedule constraints precluded a custom design; therefore the design was based on available off-the-shelf converter modules.

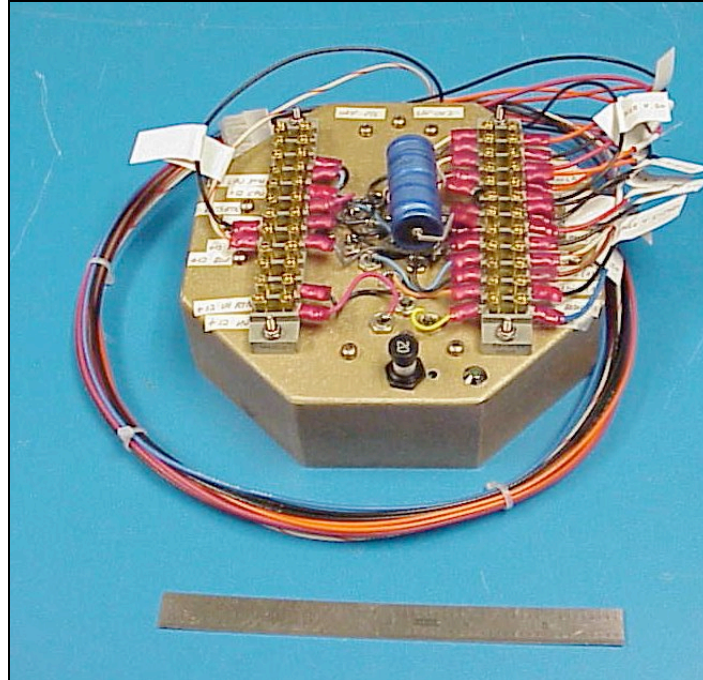


Fig. 12 Radio, RFD and Router Power supply.

The shape and dimensions of the power supply unit (see Fig. 12) were selected for the maximum available payload for a number of small airborne vehicles that were considered for potential use in the demonstrations.

A total of 9 outputs were required: 3.3 V and 5 V for both analog and digital sections, 12 V for RFD, radio and router, and low-current 24 V and -5 V for the radio. Isolation between outputs was provided for noise/ground loop minimization. Total design output power is 135 W (which includes a minimum 25% margin).

To accommodate two classes of airborne vehicles, two lightweight power supply types were designed for the FCS-C program. The light airborne (UAV) platform provides 12 V DC nominal (14-11 V, fully charge to discharged); the remaining platforms (helicopter and robots) provide 24-28 VDC nominal. A relatively small number of converter module vendors produce models capable of 12 V operation; most concentrate on the 24 V, 48 V telecom and 270 V distributed power versions. The vendor of the converter modules, Acute Power, Inc. produces versions covering both the required 9-18 V and 18-36 V specified operating ranges. This commonality facilitated overall FCS-C power system design. The 30 W rating (of the largest MAC-40 modules) satisfied the power requirements of the various individual outputs. The supply contains a total of 9 converter modules, of which 6 are the 30 W types.

Input ripple current management techniques include the use of low-parasitic (ESR/ESL) multilayer polymer capacitors directly across the inputs of most of the modules, twisted wiring to minimize coupling loop areas and a common-mode ferrite core choke. Bulkhead feed through filters are used for all input and output connections to minimize electromagnetic interference (EMI) from the converter switching processes. Input protection consists of a circuit breaker followed by an anti-reversal diode, which also provides transient voltage protection.

Supply efficiency of the 12 V power supply measured at approximately 70% of capacity is 71%. For reference, efficiency of the 24/28 V version measured at the same relative loading is 79%.

VI. □ Integration with UAV

A. UAV Description

The UAV selected for the demonstration (see Fig. 13) was built by Advanced Ceramics Research. It is a small fixed wing UAV with a 3 foot long body and a payload area of about 12" long x 10" wide x 5" high. The available payload weight is 12 pounds when the aircraft is fully fueled.



Fig. 13 UAV.

B. Mechanical Integration

Installing payloads into UAVs presents many physical challenges. Size, weight, and power are all severely limited. For its size, the UAV had a very generous payload volume and weight carrying capability, but with the complexity of the desired payload, the challenges remained.

The FCS-C program required the installation of the radio, the RFD, a network router, a video camera and processor, an antenna, a power supply, and a battery power source capable of running the system for at least one hour. A list of the component weights is given in Table 5.

Table 5 System Weight

Radio	3.7 lbs
RFD	1.6 lbs
Router	2.1 lbs
Video System	0.9 lbs
Antenna	0.4 lbs
Power Supply	1.8 lbs
Batteries	1.2 lbs
Total	11.7 lbs

The small form factor of the ADR, ADT and DPE allowed the radio to be compressed into a suitable volume package that is also low in weight. The router, power supply, and RFD were made up of commercial components that were packaged into small, light cases for mounting into the UAV. Lithium Polymer batteries were selected as the primary power source for the payload. The batteries have good power to weight ratio, and a thin, flat form factor that allowed installation into small payload spaces.

All of the components were mounted onto a removable, fiberglass tray that provided easy system installation into the payload area. The system components are shown in a mock-up of the UAV body in Fig. 14.

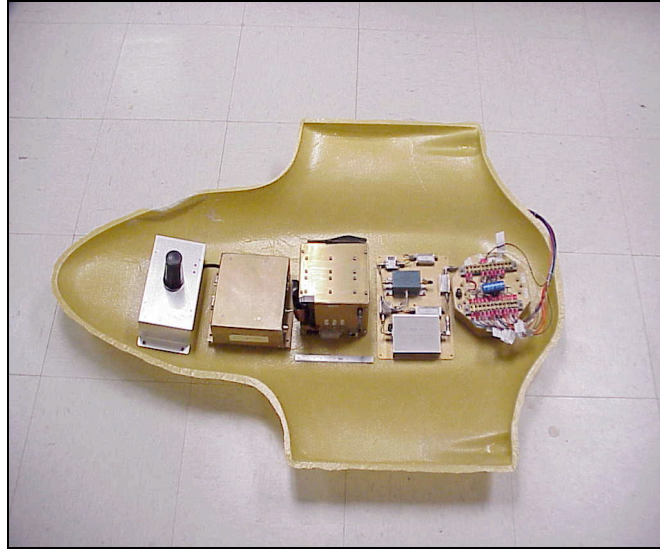


Fig. 14 UAV Payload.

C. Thermal Integration

Although the system was small, it consumed approximately 106 watts of power during transmit (see Table 6). When not in transmit mode, the PA was turned off and power consumption of the RFD was less than 1 W.

Table 6 Power Budget

Radio	37.1 W
RFD	20.0 W (during Transmit)
Router	24.9 W
Video System	8.4 W
Power Supply	16.2 W
Total	106.6 W

This presented a challenge for keeping the system cool. The solution for the FCS-C demonstration was to include a fan to circulate air within the payload area.

D. Electromagnetic Emissions

In June 2003 the radio, router, power supplies and RFD were tested with the UAV flight control system to identify any electromagnetic interference issues. The avionics, servos, ground station, control link and flight wiring harness were configured for Hardware-In-the-Loop testing.

Pre- and post-amplification filtering takes place in the RFD, which results in transmitted out-of-band spectrum that is essentially in the noise floor (see Fig. 15). This data is at full power transmit (~2 W peak), 25.6 MHz bandwidth, 100% duty cycle centered at 2.44 GHz.

The flight servo motors were placed next to the Ultra Comm antenna during 100% duty cycle, full power transmit. This resulted in almost undetectable chatter of the servos, and was considerably less chatter than that caused by the ground to air control link (900 MHz ISM band). It was determined that this effect was negligible and would not impact flight performance.



Fig. 15 Transmit Spectrum 50 MHz - 3 GHz; and 2 – 8 GHz.

Next, testing was conducted to determine if the system would interfere with the air-ground control link. Pads were placed before the ground antenna to simulate a communication link with a received signal strength indication (RSSI) of approximately -100 dBm. The 900 MHz UAV control antenna was then placed next to the Ultra Comm antenna, power supplies, radio, and router. No noticeable degradation to the link quality was observed.

VII. System Demonstration and Future Activities

A. August 2003 Demonstration

In August 2003 a system demonstration was conducted at the Orchard Training Area outside of Boise, Idaho. The demonstration consisted of 18 ground vehicles (16 SUVs, 1 robot, 1 M113), 2 helicopters, and 1 UAV. Each vehicle had an Ultra Comm system (the larger vehicles had more capabilities than the smaller system designed for the UAV). The goals of the demonstration were to show sustained high data rates in a variety of terrain and interference conditions. This marked the first demonstration of a UAV equipped with the Ultra Comm communications system. The goal for the UAV portion of the test was to demonstrate high throughput data sourcing and routing for up 1 1/2 hours (limited by fuel and battery lifetime). A number of factors, including UAV flight restrictions, weather, and range availability limited the UAV to just one flight with the Ultra Comm hardware installed. The system survived the flight and a rather rough landing; however a networking software problem prevented demonstration of full network connectivity during the flight. For the demonstration, two helicopters were also equipped with directional as well as omni antennas and higher output PAs for longer range. These successfully enabled networked communications between ground nodes over the course of the demonstration.

B. Scaling to Other Platforms

There are two general directions that we can go from here: one is to demonstrate more capability for larger UAV platforms; the other is to demonstrate smaller, lighter, lower power variants for smaller UAVs or micro air vehicles (MAV).

For larger UAVs additional viable enhancements include increasing the number of independent RF channels by mounting additional ADR, ADT and DPE cards to a PCMCIA format extension chassis. The core configuration starts with a single transmit and receive pair, but extension to two or four transmit/receive channels within a single PCI back plane is supported by the design architecture. There is no hard limit as to how many RF channels or antenna array elements can be supported. The DPE has the processing and input/output (I/O) capacity to execute advanced real-time analog and digital beamforming, and has the capacity to handle processing wide-band IF signals.

For smaller UAVs shrinking the size and power of the system can be accomplished in several ways. A Class A power amplifier is currently used in the RFD. Considerable power savings would result from using a more efficient amplifier design, at the expense of linearity. Another possibility is to get higher linearity for a given power out. Typical PA manufacturers specify a third order intercept point (IP3) that is 9 - 10 dB higher than P-1dB. However, through linearization techniques and newer high-speed processes it should be possible to get an IP3 that is perhaps ~ 16 dB higher than P-1dB. The next version of the ADR and ADT boards can implement more extensive power management to turn off unused circuits. In addition, commercial technology continually improves power vs. performance, so simply updating certain components will also save power.

VIII. Summary

An advanced, lightweight communication system for UAVs has been developed within the DARPA FCS-C program. The system offers high data rate capability in clear conditions and the option of trading data rate, range, and LPI/LPD/AJ characteristics to operate under very adverse conditions. The system has been lab tested and tested with key components of the UAV guidance and control system. No problem areas were identified. There was a network demonstration in August 2003 involving ground vehicles, helicopters and a small UAV, all equipped with Ultra Comm systems. The demonstration showed flight worthiness of the TRL 5 hardware. Further integration and testing of the system is planned in future phases of the FCS-C program, with application to other air vehicles.

References

- ¹Le, Chris, and Stuckey, Peter, "FCS Low Band Radio Development," MILCOM 2001.
- ²Mankins, John C., "Technology Readiness Levels – a White Paper," NASA Office of Space Access and Technology, April 1995.
- ³DARPA, "FCS Communications Program Solicitation, FCS Communications System Integration and Demonstration," PS01-04.
- ⁴Litwin, Louis, and Pugel, Michael, "The Principles of OFDM", *RF Design Magazine*, Jan. 2001, pp. 30-48.